ATP homeostasis underlies optimal glucose consumption by *Saccharomyces cerevisiae*

Kulika Chomvong[1], Daniel I. Benjamin[2], Daniel K. Nomura[2] and Jamie H.D. Cate[3,4,5,#]

[1]Department of Plant and Microbial Biology, University of California, Berkeley, CA 94720

[2]Department of Nutritional Sciences and Toxicology, University of California, Berkeley, CA 94720

[3]Department of Molecular and Cell Biology, University of California, Berkeley, CA 94720

[4]Department of Chemistry, University of California, Berkeley, CA 94720

[5]Physical Biosciences Division, Lawrence Berkeley National Laboratory, Berkeley, CA 94720

[#]Corresponding author (email: jcate@lbl.gov)

KC: kchomv@gmail.com

DIB: dbenjami@stanford.edu

DKN: dnomura@berkeley.edu

JHDC: jcate@lbl.gov

Running title: ATP and optimal glucose consumption

Final character count: 50,759

Keywords: cellobiose/GCN4/glucose sensors/metabolomics/PMA1

23

24 **Abstract**

25

26 Glycolysis is central to energy metabolism in most organisms, and is highly
27 regulated to enable optimal growth. In the yeast *Saccharomyces cerevisiae*, feedback
28 mechanisms that control flux through glycolysis span transcriptional control to
29 metabolite levels in the cell. Using a cellobiose consumption pathway, we decoupled
30 glucose sensing from carbon utilization, revealing new modular layers of control that
31 induce ATP consumption to drive rapid carbon fermentation. Proton pumping and
32 regulation of amino acid biosynthesis mediated by extracellular glucose sensors
33 independently contribute to maintenance of energy homeostasis. Controlling the upper
34 bound of cellular ATP levels may be a general mechanism used to regulate energy
35 levels in cells, via a regulatory network that can be uncoupled from ATP concentrations
36 under perceived starvation conditions.

37

38

38

39 ## Introduction

40 Most microorganisms favor glucose as their primary carbon source, as reflected
41 in their genetic programs hard-wired for this preference. Central to carbon metabolism is
42 glycolysis, which is finely tuned to the dynamic state of the cell due to the fact that
43 glycolysis first consumes ATP before generating additional ATP equivalents. To avoid
44 catastrophic depletion of ATP, the yeast *Saccharomyces cerevisiae* has evolved a
45 transient ATP hydrolysis futile cycle coupled to gluconeogenesis (van Heerden *et al*,
46 2014). Glycolysis in yeast is also tightly coupled to glucose transport into the cell,
47 entailing three extracellular glucose sensing mechanisms and at least one intracellular
48 glucose signaling pathway (Youk & van Oudenaarden, 2009).

49 Synthetic biology and metabolic engineering of yeast holds promise to convert
50 this microorganism into a “cell factory” to produce a wide range of chemicals derived
51 from renewable resources or those unattainable through traditional chemical routes.
52 However, many applications require tapping into metabolites involved in central carbon
53 metabolism, a daunting challenge as living cells have numerous layers of feedback
54 regulation that fine-tune growth to changing environments. Cellular regulation evolved
55 intricate networks to maintain and ensure cell survival. For example *S. cerevisiae* has
56 evolved to rapidly consume high concentrations of glucose through fermentation, while
57 repressing the expression of other carbon consumption pathways, an effect termed
58 glucose repression. When perturbed genetically, regulatory networks such as those in
59 glucose repression often generate undesirable or unexpected phenotypes.

60 For yeast to be useful in producing large volumes of renewable chemicals or
61 biofuels, it will be important to expand its carbon utilization to include multiple sugars in
62 the plant cell wall. One promising approach that helps overcome glucose repression
63 and allows simultaneous utilization of different sugars is cellobiose consumption (Ha *et*
64 *al*, 2011). Cellobiose is a disaccharide with two units of glucose linked by a ß-1,4
65 glycosidic bond. Cellobiose consumption using a minimal additional pathway in yeast—
66 a cellodextrin transporter (CDT-1) and intracellular ß-glucosidase (Galazka *et al*, 2010)–
67 avoids glucose repression by importing carbon in the form of cellobiose instead of
68 glucose. The cellodextrin transporter allows cellobiose to enter the cell where it is
69 hydrolyzed to glucose and consumed via the native glycolytic consumption pathway. By
70 moving glucose production into the cell, the *N. crassa*-derived cellobiose consumption
71 pathway is nearly the minimal synthetic biological module imaginable in *S. cerevisiae*,
72 comprised of just two genes. Nevertheless, in *S. cerevisiae* the cellobiose consumption
73 pathway is inferior to consumption of extracellular glucose in terms of rate and results in
74 a prolonged lag phase (Lin *et al*, 2014). Previous efforts to understand the impact of
75 cellobiose consumption on the physiology of *S. cerevisiae* using transcriptional profiling
76 revealed that cellobiose improperly regulates mitochondrial activity and amino acid
77 biosynthesis, both of which are tightly coupled to the transition from respiration to
78 fermentation (Lin *et al*, 2014).

79 Since glycolytic enzymes are regulated mostly at the post-transcriptional level
80 (Daran-Lapujade *et al*, 2007), we probed cellobiose consumption in *S. cerevisiae* at the
81 metabolite level. We found that key metabolites in glycolysis are highly imbalanced,
82 leading to low flux through glycolysis and slow fermentation. We also found that excess

83 ATP levels drive the imbalance, and identified a new regulatory role of glucose sensors
84 in cellular ATP homeostasis.
85

86 Results

87

88 Metabolite profiling of cellobiose utilizing *S. cerevisiae*

89 *S. cerevisiae* cells engineered with the cellobiose consumption pathway ferment
90 cellobiose more slowly than glucose and often exhibit a prolonged lag phase when
91 transitioning to consumption of this disaccharide (Lin *et al*, 2014). We hypothesized that
92 cellobiose consumption results in an ATP deficit in glycolysis relative to glucose, due to
93 the fact that the cellodextrin transporter (CDT-1) in the cellobiose utilizing pathway is a
94 proton symporter, requiring ATP hydrolysis for cellobiose uptake (Kim *et al*, 2014).
95 Moreover, under anaerobic conditions, ATP production is limited to substrate-level
96 phosphorylation, further restricting ATP availability. We measured the steady-state
97 concentrations of ATP and other metabolites in central carbon metabolism in yeast
98 fermenting cellobiose compared to glucose. Of the 48 compounds analyzed, the
99 abundance of 25 compounds was significantly different (p-value < 0.01) between
100 cellobiose and glucose-fed samples (Figure 1A). Surprisingly, ATP levels increased by
101 6-fold in the cellobiose grown cells (Figure 1B). The relative abundance of compounds
102 in glycolysis—fructose 6-phosphate (F6P), glucose 6-phosphate (G6P), glucose and
103 pyruvate—increased by 444-, 81-, 7- and 3-fold, respectively, while that of
104 phosphoenolpyruvate decreased by 2-fold (Figure 1B). These results suggest that the

105 yeast cells underwent drastic physiological changes, reflected in metabolite levels,
106 when cellobiose was provided in place of glucose.
107
108 **Phosphofructokinase-1 inhibition by excess ATP**
109 Given the dramatic buildup of glucose, G6P and F6P intermediates prior to the
110 phosphofructokinase (*PFK1*) reaction in glycolysis (Figure 2A), we reasoned that Pfk1
111 might be a major bottleneck in cellobiose consumption. Pfk1 catalyzes the
112 phosphorylation of F6P, using one ATP and yielding fructose 1,6-bisphosphate
113 (F1,6BP) as a product. As the second committed step in glycolysis, Pfk1 is heavily
114 regulated—with ATP acting as an allosteric inhibitor and AMP and fructose 2,6-
115 bisphosphate serving as activators (Bañuelos *et al*, 1977; Avigad, 1981; Nissler *et al*,
116 1983).
117 To test whether allosteric inhibition of Pfk1 by ATP limited cellobiose
118 fermentation, a mutation in Pfk1 that makes the enzyme ATP-insensitive (P722L in the
119 Pfk1 beta subunit, note the original publication referred to this mutation as P728L
120 (Rodicio *et al*, 2000)) was introduced into the chromosomally encoded *PFK1* gene
121 (mutation here termed *pfk1m*) in the cellobiose utilizing strain. This mutation was
122 previously shown to reduce ATP inhibition but also AMP and fructose 2,6-bisphosphate
123 activation of Pfk1 in *S. cerevisiae* (Rodicio *et al*, 2000). We chose this mutation over an
124 ATP-insensitive, AMP/F2,6BP-sensitive mutant phosphofructokinase (Nissler *et al*,
125 1983) because the latter's phenotype has not been evaluated in *S. cerevisiae*.
126 Consistent with allosteric inhibition of Pfk1 by ATP, the cellobiose consumption
127 efficiency (E_c) of the *pfk1m* strain increased by 33% in comparison to the strain with

128 wild-type Pfk1 (Figure 2B). Furthermore, the relative abundance of G6P and F1,6BP
129 decreased by 47% and 34%, respectively, while that of ATP remained relatively
130 unchanged (Figure 2C). These results indicate that the 6-fold increase in cellular ATP
131 concentrations allosterically inhibited Pfk1, resulting in accumulation of glucose, G6P
132 and F6P, which eventually slowed down cellobiose consumption.
133

134 **Limited activity of plasma membrane ATPase**

135 Although the *pfk1m* strain partially increased the rate of cellobiose fermentation,
136 cellular ATP remained elevated relative to glucose fermentation. It is unlikely that ATP
137 production was the cause of the difference, as fermentation is limited to substrate-level
138 phosphorylation under anaerobic conditions regardless of carbon source. We therefore
139 tested whether the activity of one of the major ATP sinks in yeast, the plasma
140 membrane ATPase (Pma1) was responsible for the ATP buildup. Pma1 hydrolyzes 25-
141 40% of cellular ATP in yeast (Gradmann *et al*, 1978) and is heavily regulated by glucose
142 (Serrano, 1983).

143 A constitutively active mutant form of *PMA1* (*pma1*-Δ916, here abbreviated *pt*)
144 (Mason *et al*, 2014) was introduced into the endogenous *PMA1* locus in the cellobiose
145 utilizing strain. This mutation results in high Pma1 ATPase activity even in carbon
146 starvation conditions (Mason *et al*, 2014). We observed a 66% decrease in cellular ATP
147 levels in the *pt* strain in comparison to the wild-type control (WT, i.e. cellobiose pathway
148 only) (Figure 2C). Phenotypically, the E_c of the mutant strain was 4 times that of the
149 control (Figure 2B). In addition, the concentrations of G6P and F1,6BP decreased by
150 58% and 93%, respectively, relative to strains expressing wild-type *PMA1*. Notably,

151 these concentrations dropped more than when the ATP-insensitive *PFK1* mutant was
152 introduced (Figure 2C). These results suggest that increased Pma1 ATPase activity
153 improved cellobiose fermentation, by alleviating ATP accumulation that allosterically
154 inhibited Pfk1 in glycolysis.

155 With decreased intracellular ATP concentrations in the *pma1*-Δ916 strain, ATP
156 inhibition at the Pfk1 step is unlikely to limit glycolysis. Consistent with this hypothesis,
157 the cellobiose consumption profile of a *pfk1m-pt* double mutant was identical to that of
158 the *pt* strain (Figure 2A). Surprisingly, the levels of G6P, F1,6BP and ATP in the double
159 mutant strain were higher than in the *pt* strain (Figure 2C). In fact, their levels were
160 similar to those in the *pfk1m* strain (Figure 2C). This may be because *pfk1m* has
161 reduced activation by AMP and fructose 2,6-bisphosphate, in addition to reduced
162 inhibition by high ATP concentrations (Rodicio *et al*, 2000). Taken together, these data
163 suggest that the effect of reduced Pfk1 allosteric activation may only be evident in the
164 absence of Pfk1 inhibition by ATP.

165

166 **Carbon starvation-like state of the plasma membrane ATPase**

167 We wondered whether the limited Pma1 activity in cellobiose-fed cells is due to
168 the absence of extracellular glucose in the media. Transcriptionally, the presence of
169 glucose increases *PMA1* mRNA levels by 2-4 times via the regulation of Rap1, Gcr1
170 and Sir2 (Rao *et al*, 1993; García-Arranz *et al*, 1994; Kang *et al*, 2015). Consistent with
171 the requirement for extracellular glucose sensing, previous RNA sequencing
172 experiments revealed a 40% decrease in *PMA1* transcript levels when cellobiose was
173 provided in place of glucose (Lin *et al*, 2014). However, although transcriptional

174 regulation of *PMA1* is important, it is slower than post-transcriptional regulation and
175 results in smaller changes (Serrano, 1983; Eraso *et al*, 2006). In the presence of
176 glucose, phosphorylation of Ser-899 decreases Pma1's K_m and Ser-911/Thr-912
177 increases Pma1's V_{max} for ATP, respectively (Serrano, 1983; Portillo *et al*, 1991; Lecchi
178 *et al*, 2007). Given the excess amount of ATP observed in cellobiose utilizing conditions
179 (Figure 1), we hypothesized that V_{max}-determining phosphorylation states of Ser-911
180 and Thr-912 might play a major role in establishing the efficiency of cellobiose
181 fermentation. We did not investigate the phosphorylation of Ser-899, because the 6-fold
182 excess of ATP likely overcame the potential problems associated with K_m values (Eraso
183 & Portillo, 1994).
184 Combinatorial mutations of Ser-911/Thr-912 to alanine and aspartic acid were
185 introduced into the endogenous *PMA1* gene to prevent or mimic phosphorylation,
186 respectively. We were unable to obtain strains with *pma1* S911A T912A and *pma1*
187 S911A T912D, potentially because the combinations were lethal. All mutant strains
188 whose Pma1 S911 position was mutated to aspartic acid consumed cellobiose more
189 efficiently in comparison to when the S911 position remained unchanged (Figure 3A).
190 By contrast, mutating Pma1 T912 to aspartic acid did not show a correlation with the
191 cellobiose consumption phenotype. These results suggest that phosphorylation of Pma1
192 at S911 was lacking when cellobiose was provided as a sole carbon source.
193
194 **Positive effects of extracellular glucose sensor deletions**
195 According to the above mutational analysis, the Pma1 phosphorylation
196 state of cellobiose-fed cells was similar to that in carbon starvation conditions (Figure

197 3B) (Lecchi *et al*, 2007). Based on the relatively high level of intracellular glucose
198 present in the cellobiose-grown cells (Figure 1), extracellular glucose is likely to be
199 essential for full activation of Pma1 through S911 phosphorylation, as high intracellular
200 glucose concentrations (Figure 1) or glucose metabolism (Rolland *et al*, 2002) was
201 unable to satisfy this role.

202 Snf3, Rgt2 and Gpr1 are the three known sensors of extracellular glucose in *S.*
203 *cerevisiae*. Snf3 and Rgt2 mainly regulate glucose transport while Gpr1 controls cell
204 physiology via an interaction with Gpa2 to activate protein kinase A and cAMP synthesis
205 (Rolland *et al*, 2002). To mimic the presence of extracellular glucose, constitutively
206 active mutations (*snf3* R229K, *rgt2* R231K and *gpa2* R273A) were introduced into the
207 endogenous loci to probe the role of each glucose-sensing pathway (Ozcan *et al*, 1996;
208 Xue *et al*, 1998). Surprisingly, the cellobiose consumption efficiency of all the three
209 mutant strains decreased by ~25% (Figure S1A). We then inverted the genetic
210 modifications by deleting *SNF3, RGT2* and/or *GPA2*. Notably, the triple glucose-sensing
211 deletion strain (*snf3*Δ*rgt2*Δ*gpa2*Δ*, or srg*Δ) showed a 275% increase in E_c (Figure 4A).

212 Combinatorial deletions revealed that the Gpr1 pathway did not contribute to
213 improved cellobiose fermentation, but combining the *SNF3* and *RGT2* deletions (*sr*Δ)
214 was necessary and sufficient to replicate the E_c of the triple deletion strain (Figure 4A,
215 Figure S1C). Consistent with the observed E_c values, the intracellular ATP levels of
216 *srg*Δ and *sr*Δ decreased by 41% and 18% respectively, while those in the individual-
217 deletion strains *snf3*Δ and *rgt2*Δ remained unchanged (Figure 4A). These results reveal
218 a negative correlation between E_c and cellular ATP levels (Figure 4B) and that Snf3 and

219 Rgt2 acted together to regulate cellular ATP levels, in addition to regulating glucose
220 transport.

221 Although the additional deletion of *GPA2* (*gpa2*Δ) in the *sr*Δ strain did not further
222 improve E_c (Fig 4A), it reduced the relative abundance of ATP by 28%, implying that the
223 Gpr1 pathway has a separate mechanism to control cellular ATP levels that does not
224 directly affect carbon metabolism. Consistently, *gpa2*Δ had a negative or neutral impact
225 on cellobiose consumption (Figure S1). The decrease in ATP level may be a result of
226 altered cellular activities, controlled by Gpr1 via the Tor and cAMP-PKA-Ras pathways
227 (Rolland *et al*, 2002). The relationship between Gpr1-regulated ATP levels and carbon
228 metabolism remains to be discovered. Since *gpa2*Δ did not have a direct effect on E_c, it
229 was not investigated further in this study.

230

231 **Snf3/Rgt2 regulation of cellular ATP levels**

232 To examine whether Snf3/Rgt2 regulated the cellular ATP level in cellobiose
233 fermentations via Pma1, an *snf3*Δ *rgt2*Δ *pma1-*Δ*916* strain (*sr*Δ*-pt*) was constructed.
234 Notably, the E_c of the *sr*Δ*-pt* strain increased more than 4 times in comparison to the
235 wild-type control (Figure 4A, C). The improvement was additive, within the range of the
236 ΔE_c summation of *sr*Δ and *pma1-*Δ*916* strains relative to wild-type (Figure 4C). Although
237 ATP levels decreased in a nearly linear fashion as a function of E_c (Figure 4B), it is not
238 presently possible to ascertain whether the *sr*Δ and *pma1-*Δ*916* mutations act entirely
239 independently due to limitations in measurement accuracy (Figure 4C).

240 To further determine the relationship between Snf3/Rgt2 and Pma1, the
241 vanadate-specific ATPase activity of Pma1 (Viegas & Sá-Correia, 1991) from different

242 strains consuming cellobiose were analyzed (Figure 5). Consistent with the
243 constitutively active nature of the *pt* mutation, the activities of Pma1 in the *pt* and *sr*Δ-*pt*
244 strains were higher than those observed in the WT or *sr*Δ strains, respectively. Notably,
245 the ATPase activitiy of Pma1 in *sr*Δ was comparable to the WT strain suggesting that
246 Snf3 and Rgt2 in combination do not regulate Pma1 transcriptionally or post-
247 translationally in a straightforward manner.
248

249 **Transcriptional impact of Snf3/Rgt2 Deletion**

250 Given the lower cellular ATP concentration (Figure 4A) but nearly unchanged
251 Pma1 ATPase activity in the *sr*Δ strain relative to WT (Figure 5), Snf3/Rgt2 likely
252 regulate ATP homeostasis through an additional mechanism other than Pma1. A
253 systems-level analysis of yeast transcriptomes from the WT, *s*Δ, *r*Δ, and *sr*Δ strains
254 identified 137 genes that were differentially expressed and unique to *sr*Δ (p-value <
255 0.001 and absolute fold change > 2 for *sr*Δ compared pairwise with WT, *s*Δ and *r*Δ)
256 (Dataset 1.3). Notably, 14 genes (10.2%) encoding ATP binding proteins and those
257 involved in ATP catabolic processes were upregulated (Figure S2, Dataset 1.4). The
258 137 genes were further categorized into five clusters (Dataset 1.5), revealing
259 upregulation of genes involved in cellular amino acid biosynthesis, metabolic processes
260 and ATP catabolic processes, and downregulation of those in phospholipid biosynthesis,
261 phospholipid metabolism, mitochondrial structure, negative regulation of
262 gluconeogenesis and translation initiation factor eIF1 (SUI1) (Dataset 1.5, Figure S2). A
263 more comprehensive analysis of genes involved in amino acid biosynthesis revealed a

264 high correlation with upregulation of Gcn4, the central transcriptional activator of genes
265 in this pathway (Figure S3, Dataset 1.7) (Moxley *et al*, 2009; Natarajan *et al*, 2001).
266

267 Discussion

268 To identify the effects of a minimal alteration to carbon metabolism in yeast, we
269 chose a cellobiose-consumption pathway composed of two genes and analyzed its
270 cellular metabolite profiles in comparison to cells provided with glucose, yeast's
271 preferred carbon source (Figure 6). Cellobiose consumption efficiency (E_c) linearly
272 correlated with ethanol production rate, while ethanol yield remained mostly unchanged
273 (Figure S4).
274 More than half of the metabolites changed abundance significantly when
275 cellobiose was provided in place of glucose. The buildup of G6P, F6P and ATP in *S.*
276 *cerevisiae* fermenting cellobiose suggested that Pfk1 was one of the bottlenecks in the
277 process. Pfk1 is subjected to complex allosteric regulation, including inhibition by ATP
278 and activation by AMP and fructose 2,6-bisphosphate (F2,6BP) (Bañuelos *et al*, 1977;
279 Avigad, 1981; Nissler *et al*, 1983). The Pfk1 bottleneck was partially relieved in cells
280 expressing an ATP/AMP/F2,6BP-insensitive *PFK1* allele, while the ATP level remained
281 elevated. These results contrast with previous studies that identified ATP depletion and
282 the buildup of fructose-1,6-bisphosphate–the metabolite immediately downstream of
283 Pfk1–as a weak link in glycolysis (van Heerden *et al*, 2014). Although we did not
284 investigate the effect of AMP and F2,6BP activation since their changes between
285 glucose and cellobiose conditions were less than 2 fold and not statistically significant

286 (p-value ≥ 0.01), it is possible that they could influence cellobiose consumption
287 efficiency.
288 Although ATP is central to a cell's energy currency, too much ATP is not
289 necessary beneficial (Pontes *et al*, 2015; Browne, 2013). In fact, we observed a
290 negative correlation between cellular ATP levels and cellobiose consumption efficiency
291 (Figure 4B). A similar correlation has been reported for glucose as a carbon source,
292 suggesting metabolic uncoupling of energy homeostasis in yeast cells (Larsson *et al*,
293 1997). We propose that intracellular glucose concentrations–generated by cellobiose
294 hydrolysis in our experiments–and glucose metabolism (Rolland *et al*, 2002) are
295 insufficient to trigger glucose activation of key metabolic pathways and enzyme activity.
296 For example, we found that the ATP-dependent proton pump Pma1 existed in a carbon-
297 starvation like state during cellobiose fermentation, and was partially responsible for the
298 aberrant accumulation of ATP. These results suggest that neither intracellular glucose
299 nor glucose metabolism are sufficient to fully activate Pma1. A previous study showed
300 the lack of phosphorylation of S899 and S911/T912 in Pma1, in a
301 hexokinase/glucokinase deletion strain (*hxk1*Δ *hxk2*Δ *glk1*Δ) provided with glucose,
302 suggesting that phosphorylation of these residues requires glucose metabolism (Mazón
303 *et al*, 2015). Together with our results, we propose that the activation of Pma1 through
304 S911 phosphorylation requires both extracellular glucose and glucose metabolism. Our
305 results reveal that the cellobiose utilization system allows uncoupling of glucose
306 metabolism and intracellular glucose from extracellular glucose signaling. Future
307 experiments will be required to reveal why ATP was not consumed by other cellular
308 processes triggered under starvation (Thomsson *et al*, 2003).

309 Cytosolic pH is also a key regulator of carbon utilization (Dechant & Peter, 2014),
310 and is likely to be impacted by the use of the proton symporter CDT-1 for cellobiose
311 import and the resulting low activity of Pma1. High cytosolic pH is necessary and
312 sufficient to activate Tor-Ras-PKA activities, which are downstream of Gpr1 glucose
313 sensing pathway (Dechant & Peter, 2014). By contrast, the proton symporter CDT-1
314 and low activity of Pma1 may result in a low cytosolic pH. However, cytosolic pH alone
315 is unlikely to determine the cellobiose consumption efficiency (E_c) as the strain with an
316 ATP/AMP/F2,6BP-insensitive *PFK1* allele showed improved E_c but unaltered cellular
317 ATP levels. Furthermore, the inactivation of the Gpr1 pathway resulted in decreased
318 cellular ATP but unaltered E_c. Glucose storage, i.e. in the form of trehalose, may be
319 interconnected through the Gpr1 pathway because Ras-cAMP activates trehalase
320 required to break down trehalose—a phenomenon observed when gluconeogenesis is
321 switched to glycolysis (Thevelein & Hohmann, 1995). Trehalose cycling has been
322 shown to lead to an imbalanced state of glycolysis (van Heerden *et al*, 2014). The
323 relationship between carbon storage and E_c will require future studies to examine this
324 relationship.

325 We also found that the well-studied extracellular glucose sensors Snf3/Rgt2
326 exhibited a novel role in cellular ATP homeostasis through an unknown mechanism,
327 which seems to be independent of the major plasma membrane ATPase Pma1.
328 Deletion of extracellular glucose sensors (Snf3/Rgt2) increased cellobiose consumption
329 efficiency and partially restored ATP levels. It is known that deletion of *SNF3* and *RGT2*
330 slows down glucose consumption (Choi *et al*, 2015), due to the inability of these strains
331 to degrade Mth1/Std1, which block the promoter regions of hexose transporters

332 required for optimal glucose import (Moriya & Johnston, 2004; Flick *et al*, 2003;
333 Lakshmanan *et al*, 2003; Jouandot *et al*, 2011). Unlike glucose, cellobiose does not
334 signal Mth1 degradation even with intact Snf3/Rgt2 (Jouandot *et al*, 2011). Thus, genes
335 downstream of Mth1 regulation, including hexose transporters, are not expected to be
336 responsible for the improved E_c and decreased cellular ATP levels observed in *sr*Δ.
337 Based on transcriptome profiling, the lack of Snf3 and Rgt2 increases ATP-requiring
338 cellular activities through regulatory nodes other than Mth1. Consistent with this model,
339 no growth defect is observed in a *mth1*Δ strain growing on glucose, suggesting that
340 Snf3/Rgt2 has additional regulatory nodes other than Mth1 (Choi *et al*, 2015).
341 Regulation of ATP levels by the combined action of Snf3 and Rgt2 seems to
342 involve transcriptional activation of amino acid biosynthetic pathways (Figure S3),
343 although Snf3 and Rgt2 are glucose sensors (Rolland *et al*, 2002). In yeast, general
344 amino acid control (GAAC) requires transcription factor Gcn4, which directly activates
345 the amino acid biosynthetic pathways, as well as pathways for vitamins associated with
346 amino acid synthesis in conditions of amino acid starvation or stress (Natarajan *et al*,
347 2001; Moxley *et al*, 2009). Notably, the transcription profile of the *srΔ* strain compared to
348 WT reveals that pathways directly regulated by Gcn4 are induced during cellobiose
349 fermentation, indicating that Gcn4 is activated in these conditions (Figure S3).
350 Interestingly, we found that patterns of transcription activation of wild-type *GCN4*
351 relative to *gcn4*Δ strains correlate highly with *srΔ* relative to WT in cellobiose
352 fermentations (correlations of 0.52 with (Moxley *et al*, 2009) and 0.68 with (Natarajan *et*
353 *al*, 2001),respectively) (Figure S3).

354 The present results indicate that Snf3 and Rgt2 repress Gcn4 levels in the
355 absence of glucose. *GCN4* mRNA levels remain unchanged in *srΔ* relative to WT,
356 indicating that Gcn4 repression by Snf3 and Rgt2 also likely occurs translationally
357 (Hinnebusch, 1997).These results come as a surprise, as previous experiments showed
358 glucose limitation induced *GCN4* mRNA translation as a starvation response (Yang *et al*,
359 2000). Glucose limitation was shown to activate *GCN4* mRNA translation by stimulating
360 Gcn2 kinase activity (Yang *et al*, 2000), which is responsible for phosphorylating
361 translation initiation factor eIF2 and depleting active ternary complexes of eIF2 with
362 initiator tRNA and GTP (Hinnebusch, 1997). By contrast, a chemical genetics approach
363 identified the kinase Snf1, the yeast homologue of human AMP-activated protein kinase
364 (AMPK), as a repressor of *GCN4* mRNA translation in conditions with a non-glucose
365 sugar and abundant amino acid availability (Shirra *et al*, 2008), conditions more in line
366 with those used here.
367 As a homolog of the important energy sensor AMPK that maintains energy
368 homeostasis in the cells (Hardie, 2011), it is tempting to speculate that Snf1 plays a role
369 in ATP regulation downstream of Snf3/Rgt2, and potentially connects to Gcn4. Snf1 is
370 required for expression of glucose-repressed genes and may be regulated by
371 mitochondrial starvation signaling (Li *et al*, 2013). Mitochondrial activation observed in
372 cellobiose fermentation compared to glucose fermentation (Lin *et al*, 2014) may be a
373 readout of the Snf1 regulation. The direct relationships between Snf3/Rgt2, Snf1, Gcn4,
374 mitochondrial activation and cellular ATP remains to be investigated.
375 One possible additional mechanism of activation of *GCN4* mRNA translation
376 could be depletion of translation initiation factor 1 (eIF1, encoded by *SUI1*). In the *srΔ*

377 strain, levels of *SUI1* mRNA decreased nearly 2.6-fold. Consistent with a direct role for
378 eIF1, previous results demonstrated that activation of *GCN4* translation decreases with
379 increased functional eIF1 levels (Hinnebusch, 1997; Herrmannová *et al*, 2012). Notably,
380 *SUI1* transcript levels were also lower in *GCN4* cells when compared to *gcn4Δ* strains in
381 starvation conditions (Natarajan *et al*, 2001). Future experiments will be required to
382 demonstrate a direct link between eIF1 levels and *GCN4* mRNA translation activation.
383 The present systems-level study of a minimal synthetic biology pathway for
384 cellobiose consumption revealed the dramatic impact of decoupling extracellular and
385 intracellular glucose sensing, resulting in an overabundance of ATP in cells. The
386 inability of *S. cerevisiae* to catabolize ATP for cellular processes in the presence of
387 intracellular glucose and glucose metabolism but in the absence of extracellular glucose
388 resulted in slow fermentation. Thus, ATP levels must be kept in a relatively narrow
389 range for optimal fermentation and to allow robust startup of glycolysis, yet yeast seems
390 to lack a direct mechanism to monitor ATP concentrations. For example, a dynamic
391 model showed that a small concentration difference of inorganic phosphate, a product
392 of ATP hydrolysis, could alter cell fate from a stable glycolytic steady state to an
393 imbalanced dead-end state (van Heerden *et al*, 2014). Here, we found that the
394 extracellular glucose sensing by Snf3/Rgt2 required for optimal glucose fermentation
395 (Youk & van Oudenaarden, 2009) can be uncoupled from the role of these receptors in
396 regulating ATP homeostasis under carbon starvation conditions. It will be important in
397 the future to map the fully regulatory pathways of ATP homeostasis leading from
398 Snf3/Rgt2 and, independently, terminating in Pma1, along with the mechanisms

399 connecting carbon utilization to the translation of the master transcriptional regulator
400 Gcn4.
401

402 Materials & Methods

403

404 Yeast strains, media and anaerobic fermentation

405 The *S. cerevisiae* background strain used in this study was S288C *ura3::*P_{PGK1}-
406 *cdt-1* N209S/F262Y-T_{ADH1} *lyp1::*P_{TDH3}*-gh1-1 (codon optimized)-*T_{CYC1} derived by
407 chromosomal DNA library selection (Ryan *et al*, 2014). The strain was subjected to
408 further modifications using the CRISPRm system (Ryan *et al*, 2014). The list of strains
409 constructed, CRISPRm guides and primers used are included in Table S1.
410 Seed cultures for cellobiose fermentation experiments were grown in 20 g/L
411 glucose modified optimal minimal media (oMM) (Lin *et al*, 2014) and harvested at mid-
412 log phase. All cellobiose fermentation experiments were conducted under strict
413 anaerobic conditions, in 80 g/L cellobiose oMM media at an initial OD_{600} of 20, using 10
414 mL serum flasks containing 5 mL fermentation in 2-5 biological replicates. The flasks
415 were incubated at 30°C, 220 rpm. The cellobiose consumption efficiency (E_c) was
416 defined as the inverse of the area under the curve of extracellular cellobiose
417 concentration over time.
418

419 Analytical analysis of yeast metabolites

420 Extracellular cellobiose concentrations were determined by high performance
421 liquid chromatography on a Prominence HPLC (Shimadzu, Kyoto, Japan) equipped with

422 Rezex RFQ-FastAcid H 10 x 7.8 mm column. The column was eluted with 0.01 N of
423 H_2SO_4 at a flow rate of 1 mL/min, 55°C.
424 For the metabolite profiling comparison between glucose and cellobiose
425 (modified from (Benjamin *et al*, 2014)) , equal amounts of yeast cells at mid-exponential
426 phase of anaerobic sugar consumption (10 g/L cellobiose or glucose) were harvested
427 (final pellet OD_{600} equivalent to 5). The samples were quenched in 180 µL of 40:40:20
428 acetonitrile:methanol:water. Following the addition of 10 nmols of d3 serine (as an
429 internal standard), the mixtures were vortexed and centrifuged at 13,000 rpm for 10
430 minutes. The supernatants were injected onto an Agilent 6460 QQQ LC-MS/MS and the
431 chromatography was achieved by normal phase separation with a Luna NH_2 column
432 (Phenomenex) starting with 100% acetonitrile with a gradient to 100% 95:5 water
433 acetonitrile. 0.1% formic acid or 0.2% ammonium hydroxide with 50 mM ammonium
434 acetate was added to assist with ionization in positive and negative ionization mode,
435 respectively. Five biological replicates were used for each sample analyzed.
436 For targeted intracellular metabolite comparisons, yeast cells equivalent to 20
437 OD_{600} units were harvested and filtered through a 0.8 µm nylon membrane, prewashed
438 with 3 mL water, followed by another 3 mL water wash after cell filtration. The
439 membranes were placed in 1.5 mL extraction solution (0.1 M formic acid, 15.3 M
440 acetonitrile) flash-frozen in liquid nitrogen, and stored at -80°C. Before analysis, the
441 extracts were vortexed for 15 minutes and centrifuged to collect the supernatants at 4°C.
442 Glucose 6-phosphate and fructose 1,6-bisphosphate were separated and identified
443 using a 1200 Series liquid chromatography instrument (Agilent Technologies, Santa
444 Clara, CA). 1 µL of each sample was injected onto an Agilent Eclipse XDB-C18 (2.1 mm

445 i.d., 150 mm length, 3.5 µm particle size) column with a Zorbax SB-C8 (2.1 mm i.d.,
446 12.5 mm length, 5 µm particle size) guard column and eluted at 25 °C and a flow rate of
447 0.2 mL/min with the following gradient (modification from (Luo *et al*, 2007)): 15 min
448 isocratic 100% buffer A (10 mM tributylamine/15 mM acetic acid), then in 15 min with a
449 linear gradient to 60% buffer B (methanol), 2 min isocratic 60% B, then 10 min
450 equilibration with 100% buffer A. The eluent from the column was introduced into a
451 mass spectrometer for 25 minutes after the first 10 minutes. Mass spectrometry (MS)
452 was performed on an LTQ XL ion trap instrument (Thermo Fisher Scientific, San Jose,
453 CA) with an ESI source operated in negative ion mode. The MS settings were capillary
454 temperature 350 °C, ion spray voltage 4.5 kV, sheath gas flow: 60 (arbitrary units),
455 auxiliary gas flow 10 (arbitrary units), sweep gas flow 5 (arbitrary units). For the MS/MS
456 product ion scan, the scan range was m/z 80 to m/z 300. The compounds G6P at m/z
457 259.1 and F16BP at m/z 339.1 were isolated with an m/z 2 isolation width and
458 fragmented with a normalized collision-induced dissociation energy setting of 35% and
459 with an activation time of 30 ms and an activation Q of 0.250.
460

461 **Plasma membrane isolation**

462 Strains were subjected to cellobiose fermentation under anaerobic conditions.
463 Yeast cells with an OD_{600} equivalent to 40 were harvested at mid-log phase and flash
464 frozen in liquid nitrogen. Membrane fractions were extracted based on the protocol
465 published in (Kaiser *et al*, 2002).
466

467 **Pma1 ATPase activity assay**

468 The ATPase assay described in (Viegas & Sá-Correia, 1991) was modified as
469 follows. 30 µg of the isolated membrane fraction was incubated in assay buffer (50 mM
470 MES pH 5.7, 10 mM $MgSO_4$, 50 mM KCl, 5 mM NaN_3, 50 mM KNO_3) with and without 3
471 mM orthovanadate for 25 minutes at 30 °C. 1.8 mM ATP was added to start the 100 uL
472 reactions. The reactions were incubated at 30 °C for 15 minutes, then the membranes
473 were isolated from the reactions by centrifugation at 13,000x g for 10 minutes at 4°C.
474 The released inorganic phosphate was measured in the supernatant using the
475 ATPase/GTPase Activity Assay Kit (Sigma-Aldrich) based on the manufacturer's
476 protocol. The specific Pma1 ATPase activities were calculated by subtracting the
477 concentration of released inorganic phosphate in reactions provided with orthovanadate
478 from those without.
479
480 **RNA Sequencing**
481 Total RNA was extracted from yeast cells equivalent to 40 OD_{600} units harvested
482 at mid exponential phase by the RiboPure Yeast kit (Thermo Fisher Scientific).
483 Multiplexed libraries were then derived from the total RNA using TruSeq RNA Library
484 Preparation Kits v2 (Illumina Sequencing). The quality of the library was evaluated by
485 Agilent Bioanalyzer 2000 (Functional Genomics Laboratory, UC Berkeley) and
486 sequenced with Illumina HiSeq2500 RAPID platform (Vincent J. Coates Genomic
487 Sequencing Laboratory, UC Berkeley). The reads were assembled and analyzed in
488 CLC Genomics Workbench 9 (Denmark). RPKM (Reads Per Kilobase of exon model
489 per Million mapped reads) was chosen as the expression value output, which was

490 further normalized by the total expression values in a sample. Functional classification
491 was performed using FunSpec (Robinson *et al*, 2002).
492

493 **Yeast cell-based cellobiose uptake assay**

494 The cell-based cellobiose uptake assay was modified from (Li *et al*, 2015). Yeast
495 strains were grown to mid-exponential phase in 2% oMM glucose, washed with assay
496 buffer (5 mM MES, 100 mM NaCl, pH 6.0) three times and resuspended to a final OD_{600}
497 of 10. Equal volumes of the cell suspension and 200 μM cellobiose were mixed to start
498 the reactions, which were incubated at 30°C with continuous shaking for 15 minutes.
499 The reactions were stopped by adding 150 μL of supernatants to 150 μL 0.1 M NaOH.
500 The concentrations of the remaining cellobiose were measured using an ICS-3000 Ion
501 Chromatography System (Dionex, Sunnyvale, CA, USA) equipped with a CarboPac®
502 PA200 carbohydrate column. The column was eluted with a NaOAc gradient in 100 mM
503 NaOH at a flow rate of 0.4 mL/min, 30°C.
504

505 **Acknowledgements**

506 The authors thank Dr. Xin Li, Dr. Ligia Acosta-Sampson, Dr. Yuping Lin and Dr.
507 Matt Shurtleff for helpful discussions. This work was supported by funding from Energy
508 Biosciences Institute to JHDC and from National Institutes of Health (R01CA172667) to
509 DKN.
510

511 **Conflict of Interest**

512 The authors declare that they have no conflict of interest.

513 **Author contributions**

514 All authors contributed to the design of the experiments. KC and DIB carried out the
515 experiments. DKN and JHDC aided in interpretation of the systems-level experiments.
516 KC wrote the manuscript, with editing from DIB, DKN, and JDHC.

517

518 ## References:

519 Avigad G (1981) Stimulation of yeast phosphofructokinase activity by fructose 2,6-
520 bisphosphate. *Biochem. Biophys. Res. Commun.* **102:** 985–991

521 Bañuelos M, Gancedo C & Gancedo JM (1977) Activation by phosphate of yeast
522 phosphofructokinase. *J. Biol. Chem.* **252:** 6394–6398

523 Benjamin DI, Louie SM, Mulvihill MM, Kohnz RA, Li DS, Chan LG, Sorrentino A,
524 Bandyopadhyay S, Cozzo A, Ohiri A, Goga A, Ng S-W & Nomura DK (2014) Inositol
525 phosphate recycling regulates glycolytic and lipid metabolism that drives cancer
526 aggressiveness. *ACS Chem. Biol.* **9:** 1340–1350

527 Browne SE (2013) When too much ATP is a bad thing: a pivotal role for P2X7 receptors
528 in motor neuron degeneration. *J. Neurochem.* **126:** 301–304

529 Choi K-M, Kwon Y-Y & Lee C-K (2015) Disruption of Snf3/Rgt2 glucose sensors
530 decreases lifespan and caloric restriction effectiveness through Mth1/Std1 by
531 adjusting mitochondrial efficiency in yeast. *FEBS Lett.* **589:** 349–357

532 Daran-Lapujade P, Rossell S, van Gulik WM, Luttik MAH, de Groot MJL, Slijper M,
533 Heck AJR, Daran J-M, de Winde JH, Westerhoff HV, Pronk JT & Bakker BM (2007)
534 The fluxes through glycolytic enzymes in Saccharomyces cerevisiae are
535 predominantly regulated at posttranscriptional levels. *Proceedings of the National*
536 *Academy of Sciences* **104:** 15753–15758

537 Dechant R & Peter M (2014) Cytosolic pH: A conserved regulator of cell growth? *Mol*
538 *Cell Oncol* **1:** e969643–4

539 Eraso P & Portillo F (1994) Molecular mechanism of regulation of yeast plasma
540 membrane H(+)-ATPase by glucose. Interaction between domains and identification
541 of new regulatory sites. *J. Biol. Chem.* **269:** 10393–10399

542 Eraso P, Mazón MJ & Portillo F (2006) Yeast protein kinase Ptk2 localizes at the
543 plasma membrane and phosphorylates in vitro the C-terminal peptide of the H+-
544 ATPase. *Biochimica et Biophysica Acta (BBA) - Biomembranes* **1758:** 164–170
545 Available at: http://www.sciencedirect.com/science/article/pii/S0005273606000125

546 Flick KM, Spielewoy N, Kalashnikova TI, Guaderrama M, Zhu Q, Chang H-C &
547 Wittenberg C (2003) Grr1-dependent inactivation of Mth1 mediates glucose-induced
548 dissociation of Rgt1 from HXT gene promoters. *Molecular Biology of the Cell* **14:**
549 3230–3241

550 Galazka JM, Tian C, Beeson WT, Martinez B, Glass NL & Cate JHD (2010) Cellodextrin
551 transport in yeast for improved biofuel production. *Science* **330:** 84–86

552 García-Arranz M, Maldonado AM, Mazón MJ & Portillo F (1994) Transcriptional control
553 of yeast plasma membrane H(+)-ATPase by glucose. Cloning and characterization
554 of a new gene involved in this regulation. *J. Biol. Chem.* **269:** 18076–18082

555 Gradmann D, Hansen UP, Long WS, Slayman CL & Warncke J (1978) Current-voltage
556 relationships for the plasma membrane and its principal electrogenic pump in
557 Neurospora crassa: I. Steady-state conditions. *J. Membr. Biol.* **39:** 333–367

558 Ha S-J, Galazka JM, Kim SR, Choi J-H, Yang X, Seo J-H, Glass NL, Cate JHD & Jin Y-
559 S (2011) Engineered Saccharomyces cerevisiae capable of simultaneous cellobiose
560 and xylose fermentation. *Proc. Natl. Acad. Sci. U.S.A.* **108:** 504–509

561 Hardie DG (2011) AMP-activated protein kinase: an energy sensor that regulates all
562 aspects of cell function. *Genes Dev.* **25:** 1895–1908

563 Herrmannová A, Daujotyte D, Yang J-C, Cuchalová L, Gorrec F, Wagner S, Dányi I,
564 Lukavsky PJ & Valásek LS (2012) Structural analysis of an eIF3 subcomplex
565 reveals conserved interactions required for a stable and proper translation pre-
566 initiation complex assembly. *Nucleic Acids Res.* **40:** 2294–2311

567 Hinnebusch AG (1997) Translational regulation of yeast GCN4. A window on factors
568 that control initiator-trna binding to the ribosome. *J. Biol. Chem.* **272:** 21661–21664

569 Jouandot D, Roy A & Kim J-H (2011) Functional dissection of the glucose signaling
570 pathways that regulate the yeast glucose transporter gene (HXT) repressor Rgt1. *J.*
571 *Cell. Biochem.* **112:** 3268–3275

572 Kaiser CA, Chen EJ & Losko S (2002) Subcellular fractionation of secretory organelles.
573 *Meth. Enzymol.* **351:** 325–338

574 Kang WK, Kim YH, Kang HA, Kwon K-S & Kim J-Y (2015) Sir2 phosphorylation through
575 cAMP-PKA and CK2 signaling inhibits the lifespan extension activity of Sir2 in yeast.
576 *Elife* **4:**

577 Kim H, Lee W-H, Galazka JM, Cate JHD & Jin Y-S (2014) Analysis of cellodextrin
578 transporters from Neurospora crassa in Saccharomyces cerevisiae for cellobiose
579 fermentation. *Appl. Microbiol. Biotechnol.* **98:** 1087–1094

580 Lakshmanan J, Mosley AL & Ozcan S (2003) Repression of transcription by Rgt1 in the
581 absence of glucose requires Std1 and Mth1. *Curr. Genet.* **44:** 19–25

582 Larsson C, Nilsson A, Blomberg A & Gustafsson L (1997) Glycolytic Flux Is
583 Conditionally Correlated with ATP Concentration in. *J. Bacteriol.* **179:** 7243–7250

584 Lecchi S, Nelson CJ, Allen KE, Swaney DL, Thompson KL, Coon JJ, Sussman MR &
585 Slayman CW (2007) Tandem phosphorylation of Ser-911 and Thr-912 at the C
586 terminus of yeast plasma membrane H+-ATPase leads to glucose-dependent
587 activation. *J. Biol. Chem.* **282:** 35471–35481

588 Li L, Chen Y & Gibson SB (2013) Starvation-induced autophagy is regulated by
589 mitochondrial reactive oxygen species leading to AMPK activation. *Cell. Signal.* **25:**
590 50–65

591 Li X, Yu VY, Lin Y, Chomvong K, Estrela R, Park A, Liang JM, Znameroski EA, Feehan
592 J, Kim SR, Jin Y-S, Glass NL & Cate JHD (2015) Expanding xylose metabolism in
593 yeast for plant cell wall conversion to biofuels. *Elife* **4:**

594 Lin Y, Chomvong K, Acosta-Sampson L, Estrela R, Galazka JM, Kim SR, Jin Y-S &
595 Cate JH (2014) Leveraging transcription factors to speed cellobiose fermentation by
596 Saccharomyces cerevisiae. *Biotechnology for Biofuels* **7:** 126

597 Luo B, Groenke K, Takors R, Wandrey C & Oldiges M (2007) Simultaneous
598 determination of multiple intracellular metabolites in glycolysis, pentose phosphate
599 pathway and tricarboxylic acid cycle by liquid chromatography-mass spectrometry. *J*
600 *Chromatogr A* **1147:** 153–164

601 Mason AB, Allen KE & Slayman CW (2014) C-terminal truncations of the
602 Saccharomyces cerevisiae PMA1 H+-ATPase have major impacts on protein
603 conformation, trafficking, quality control, and function. *Eukaryotic Cell* **13:** 43–52

604 Mazón MJ, Eraso P & Portillo F (2015) Specific phospho-antibodies reveal two
605 phosphorylation sites in yeast Pma1 in response to glucose. *FEMS Yeast Res.*

606 Moriya H & Johnston M (2004) Glucose sensing and signaling in Saccharomyces
607 cerevisiae through the Rgt2 glucose sensor and casein kinase I. *Proceedings of the*
608 *National Academy of Sciences* **101:** 1572–1577

609 Moxley JF, Jewett MC, Antoniewicz MR, Villas-Boas SG, Alper H, Wheeler RT, Tong L,
610 Hinnebusch AG, Ideker T, Nielsen J & Stephanopoulos G (2009) Linking high-
611 resolution metabolic flux phenotypes and transcriptional regulation in yeast
612 modulated by the global regulator Gcn4p. *Proc. Natl. Acad. Sci. U.S.A.* **106:** 6477–
613 6482

614 Natarajan K, Meyer MR, Jackson BM, Slade D, Roberts C, Hinnebusch AG & Marton
615 MJ (2001) Transcriptional profiling shows that Gcn4p is a master regulator of gene
616 expression during amino acid starvation in yeast. *Mol. Cell. Biol.* **21:** 4347–4368

617 Nissler K, Otto A, Schellenberger W & Hofmann E (1983) Similarity of activation of
618 yeast phosphofructokinase by AMP and fructose-2,6-bisphosphate. *Biochem.*

619 *Biophys. Res. Commun.* **111:** 294–300

620 Ozcan S, Dover J, Rosenwald AG, Wolfl S & Johnston M (1996) Two glucose
621 transporters in Saccharomyces cerevisiae are glucose. *Proceedings of the National*
622 *Academy of Sciences* **93:** 12428–12432

623 Pontes MH, Sevostyanova A & Groisman EA (2015) When Too Much ATP Is Bad for
624 Protein Synthesis. *J. Mol. Biol.* **427:** 2586–2594

625 Portillo F, Eraso P & Serrano R (1991) Analysis of the regulatory domain of yeast
626 plasma membrane H+-ATPase by directed mutagenesis and intragenic suppression.
627 *FEBS Lett.* **287:** 71–74

628 Rao R, Drummond-Barbosa D & Slayman CW (1993) Transcriptional regulation by
629 glucose of the yeast PMA1 gene encoding the plasma membrane H(+)-ATPase.
630 *Yeast* **9:** 1075–1084

631 Robinson MD, Grigull J, Mohammad N & Hughes TR (2002) FunSpec: a web-based
632 cluster interpreter for yeast. *BMC Bioinformatics* **3:** 35

633 Rodicio R, Strauss A & Heinisch JJ (2000) Single point mutations in either gene
634 encoding the subunits of the heterooctameric yeast phosphofructokinase abolish
635 allosteric inhibition by ATP. *J. Biol. Chem.* **275:** 40952–40960

636 Rolland F, Winderickx J & Thevelein JM (2002) Glucose-sensing and -signalling
637 mechanisms in yeast. *FEMS Yeast Res.* **2:** 183–201

638 Ryan OW, Skerker JM, Maurer MJ, Li X, Tsai JC, Poddar S, Lee ME, DeLoache W,
639 Dueber JE, Arkin AP & Cate JHD (2014) Selection of chromosomal DNA libraries
640 using a multiplex CRISPR system. *Elife* **3:**

641 Serrano R (1983) In vivo glucose activation of the yeast plasma membrane ATPase.
642 *FEBS Lett.* **156:** 11–14

643 Shirra MK, McCartney RR, Zhang C, Shokat KM, Schmidt MC & Arndt KM (2008) A
644 chemical genomics study identifies Snf1 as a repressor of GCN4 translation. *J. Biol.*
645 *Chem.* **283:** 35889–35898

646 Thevelein JM & Hohmann S (1995) Trehalose synthase: guard to the gate of glycolysis
647 in yeast? *Trends Biochem. Sci.* **20:** 3–10

648 Thomsson E, Larsson C, Albers E, Nilsson A, Franzén CJ & Gustafsson L (2003)
649 Carbon starvation can induce energy deprivation and loss of fermentative capacity
650 in Saccharomyces cerevisiae. *Appl. Environ. Microbiol.* **69:** 3251–3257

651 van Heerden JH, Wortel MT, Bruggeman FJ, Heijnen JJ, Bollen YJM, Planque R,
652 Hulshof J, O'Toole TG, Wahl SA & Teusink B (2014) Lost in Transition: Start-Up of
653 Glycolysis Yields Subpopulations of Nongrowing Cells. *Science* **343:** 1245114–

654 1245114 Available at: http://www.sciencemag.org/cgi/doi/10.1126/science.1245114

655 Viegas CA & Sá-Correia I (1991) Activation of plasma membrane ATPase of
656 Saccharomyces cerevisiae by octanoic acid. *J. Gen. Microbiol.* **137:** 645–651

657 Xue Y, Batlle M & Hirsch JP (1998) GPR1 encodes a putative G protein-coupled
658 receptor that associates with the Gpa2p Galpha subunit and functions in a Ras-
659 independent pathway. *EMBO J.* **17:** 1996–2007

660 Yang R, Wek SA & Wek RC (2000) Glucose limitation induces GCN4 translation by
661 activation of Gcn2 protein kinase. *Mol. Cell. Biol.* **20:** 2706–2717

662 Youk H & van Oudenaarden A (2009) Growth landscape formed by perception and
663 import of glucose in yeast. *Nature* **462:** 875–879

664

665

665 ## Figure Legends

666 **Figure 1. Metabolite profile of cells provided with glucose or cellobiose.** (A)
667 Heatmap representation of steady state intracellular metabolite abundance of cells
668 provided with glucose or cellobiose under anaerobic conditions. Shown are the results
669 of 5 biological replicates. * identified compounds that were significantly different
670 between glucose and cellobiose conditions (p-value < 0.01) (B) Significant changes of
671 intracellular metabolite levels in cells provided with cellobiose compared to cells
672 provided glucose as a sole carbon source (p-value < 0.01 and fold-change >2, five
673 biological replicates).

674 **Figure 2. Manipulation of phosphofructokinase (*PFK1*) and plasma membrane**
675 **ATPase *(PMA1*).** (A) Schematic representation of cellobiose consumption route in the
676 upper glycolytic pathway. Glc, G6P, F6P and ATP are highlighted, and were found in
677 higher abundance when cellobiose was provided in comparison to glucose. (B)
678 Cellobiose consumption profile of the strains with ATP-insensitive Pfk1 (*pfk1m*),
679 constitutively active Pma1 (*pt*) and the combination of both mutations (*pfk1m-pt*) in
680 comparison to the cellobiose pathway-only strain, here used as wild-type (WT). (C)
681 Relative abundance of G6P, F1,6BP and ATP levels of the WT, *pfk1m, pt* and *pfk1m-pt*
682 strains, relative to the WT strain fermenting cellobiose. The experiments were carried
683 out in 5 biological replicates, with standard errors from the mean shown.

684 **Figure 3. Carbon starvation-like state of the plasma membrane ATPase (*PMA1*) in**
685 **cellobiose-fermenting cells.** (A) Cellobiose consumption efficiency (E_c) of cells
686 expressing Pma1 with phosho-mimic or phosphorylation-preventing mutations at

687 positions serine 911 (S911) and threonine 912 (T912). Shown are the mean and
688 standard deviation for 3 biological replicates. (B) Phosphorylation states of Pma1 S911
689 and T912 under carbon starvation, glucose metabolizing and cellobiose metabolizing
690 conditions. The experiments were carried out in 2 biological replicates, with standard
691 errors from the mean shown.

692 **Figure 4. Effect of glucose sensor deletions.** (A) Cellobiose consumption efficiency
693 (E_c) and cellular ATP levels of strains with different glucose sensor deletions and
694 different combinations of constitutively-active Pma1 mutations. Shown are the averages
695 and standard deviations of three biological replicates. (B) Correlation of E_c and cellular
696 ATP. Standard deviations for three biological replicates are shown for each point. (C)
697 Additive effect of the increase in E_c and the decrease in cellular ATP of *sr*Δ and *pt* in
698 *sr*Δ-*pt* strain. The experiments were carried out in 5 biological replicates, with standard
699 errors form the mean shown.

700 **Figure 5. ATPase activity of the plasma membrnae ATPase Pma1.** Specific Pma1
701 ATPase of WT*, pt, sr*Δ and *sr*Δ-*pt* strains measured from normalized membrane
702 fractions of cells harvested at mid-log phase. The experiments were carried out in 3
703 biological replicates, with standard errors from the mean shown.

704 **Figure 6. Schematic representation of ATP homeostasis and cellular regulation of**
705 **cellobiose fermentation.** Excess ATP inhibited phosphofructokinase (Pfk1), resulting
706 in an upper glycolytic metabolite buildup and slow cellobiose consumption. The buildup
707 of ATP may be caused by low activity of Pma1, with no phosphorylation at position 911.
708 Additionally, glucose sensors Snf3 and Rgt2 together influenced cellular ATP levels via

709 Gcn4-regulated amino acid biosynthesis.

710

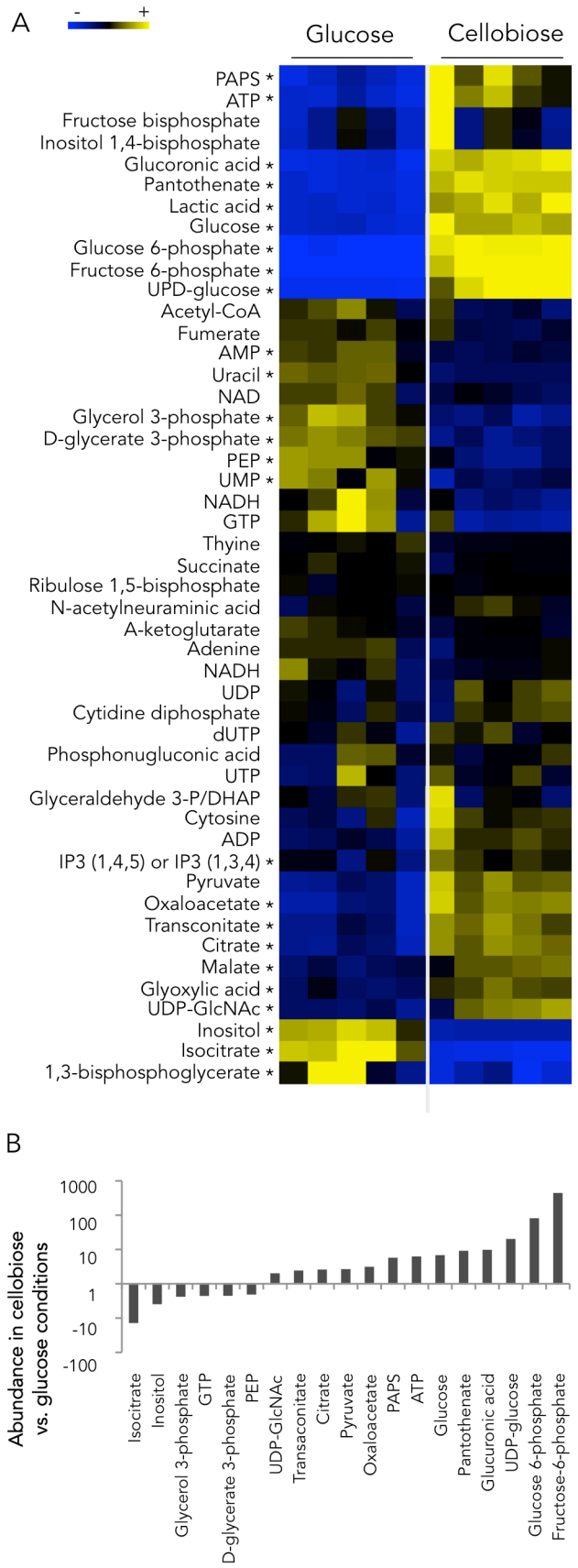
A
-
+
Glucose
Cellobiose
PAPS *
ATP *
Fructose bisphosphate
Inositol 1,4-bisphosphate
Glucoronic acid *
Pantothenate *
Lactic acid *
Glucose *
Glucose 6-phosphate *
Fructose 6-phosphate *
UPD-glucose *
Acetyl-CoA
Fumerate
AMP *
Uracil *
NAD
Glycerol 3-phosphate *
D-glycerate 3-phosphate *
PEP *
UMP *
NADH
GTP
Thyine
Succinate
Ribulose 1,5-bisphosphate
N-acetylneuraminic acid
A-ketoglutarate
Adenine
NADH
UDP
Cytidine diphosphate
dUTP
Phosphonugluconic acid
UTP
Glyceraldehyde 3-P/DHAP
Cytosine
ADP
IP3 (1,4,5) or IP3 (1,3,4) *
Pyruvate
Oxaloacetate *
Transconitate *
Citrate *
Malate *
Glyoxylic acid *
UDP-GlcNAc *
Inositol *
Isocitrate *
1,3-bisphosphoglycerate *
B
Abundance in cellobiose vs. glucose conditions
1000
100
10
1
-10
-100
Isocitrate
Inositol
Glycerol 3-phosphate
GTP
D-glycerate 3-phosphate
PEP
UDP-GlcNAc
Transaconitate
Citrate
Pyruvate
Oxaloacetate
PAPS
ATP
Glucose
Pantothenate
Glucuronic acid
UDP-glucose
Glucose 6-phosphate
Fructose-6-phosphate

710

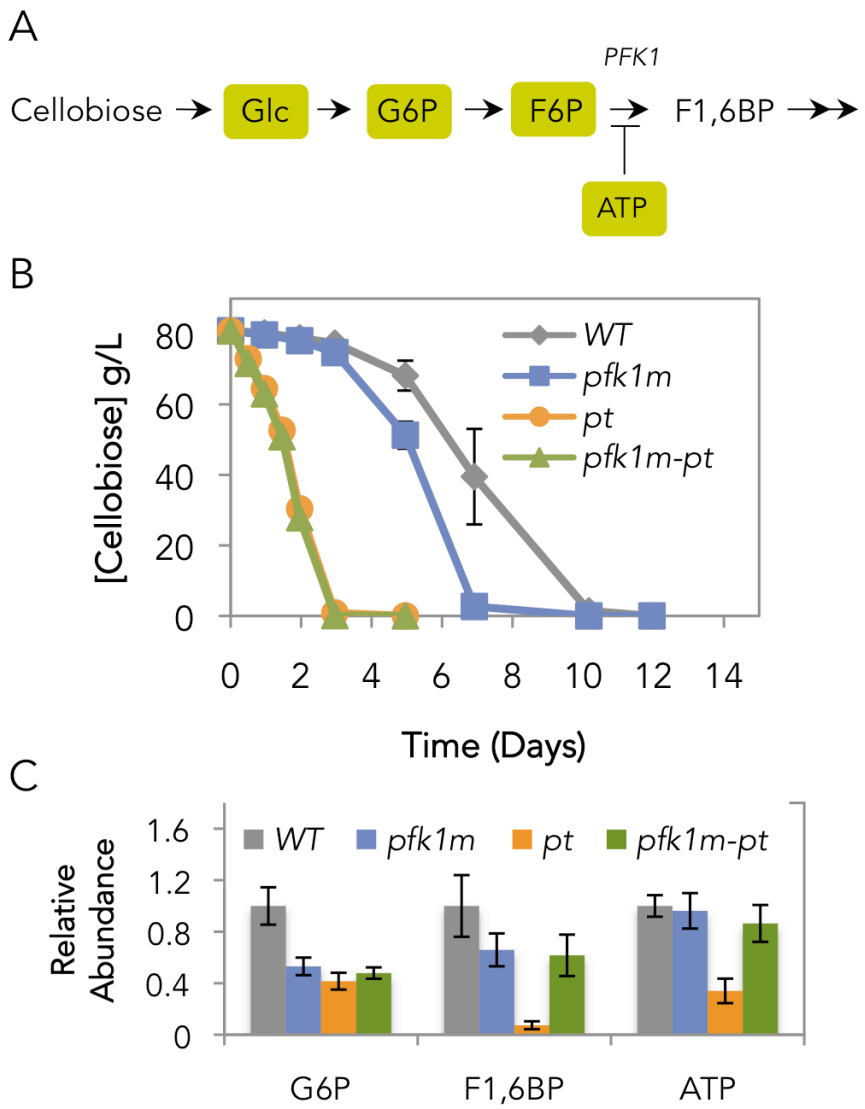
A
PFK1
Cellobiose
Glc
G6P
F6P
F1,6BP
ATP
B
[Cellobiose] g/L
80
60
40
20
0
0
2
4
6
8
10
12
14
Time (Days)
WT
pfk1m
pt
pfk1m-pt
C
Relative Abundance
1.6
1.2
0.8
0.4
0
WT
pfk1m
pt
pfk1m-pt
G6P
F1,6BP
ATP

711
712

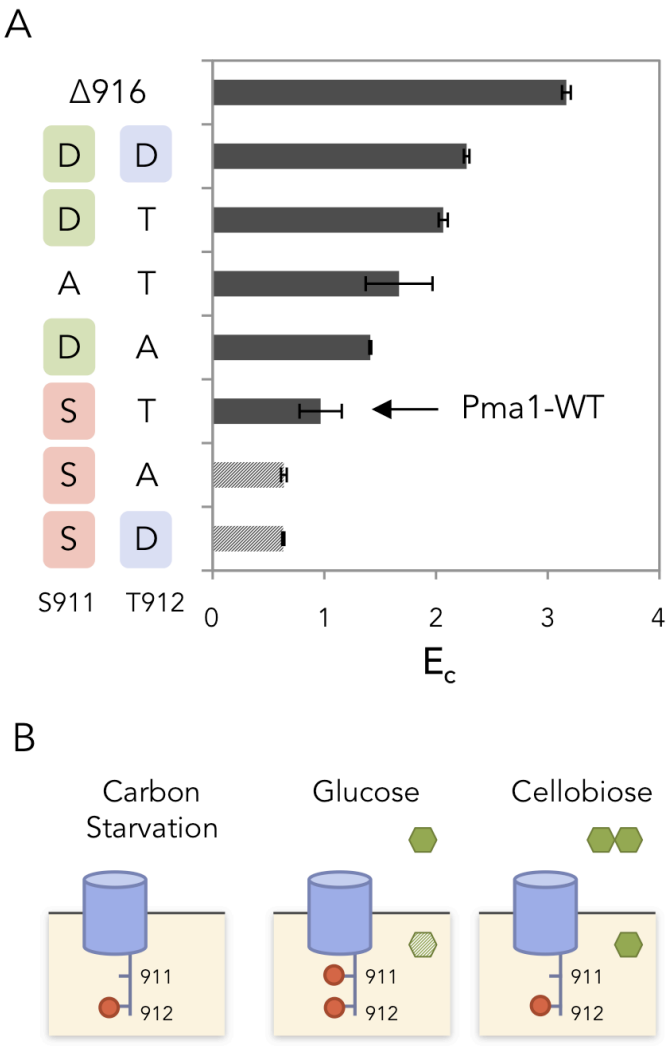
A
Δ916
D D
D T
A T
D A
S T
S A
S D
S911 T912
Pma1-WT
0 1 2 3 4
E_c
B
Carbon Starvation
Glucose
Cellobiose
911
912

712
713

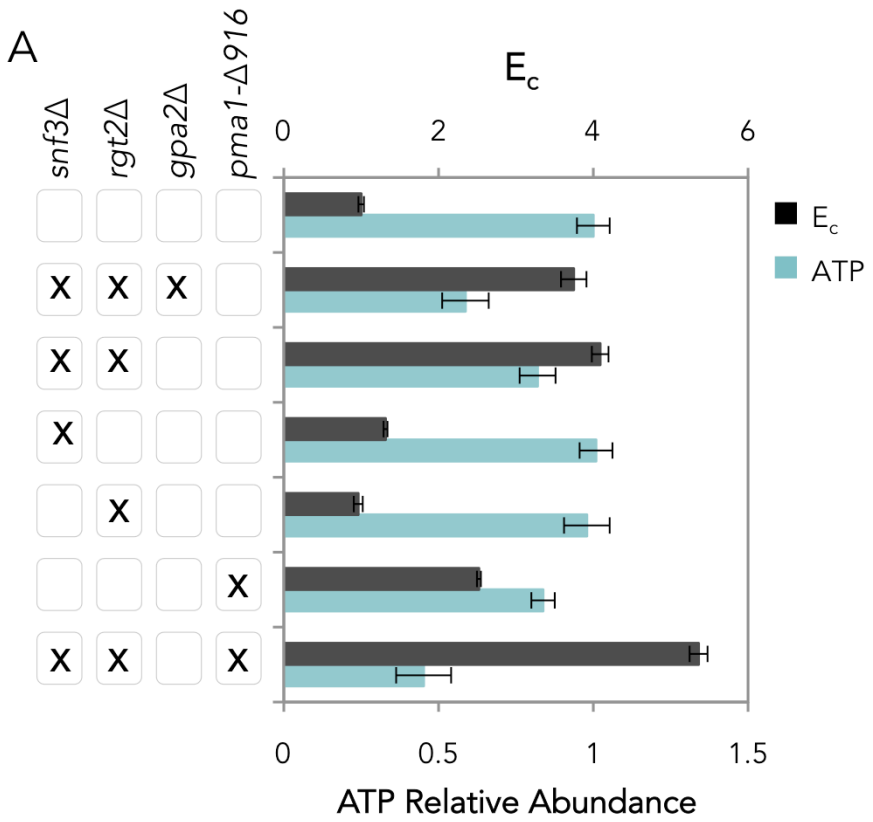
A
snf3Δ
rgt2Δ
gpa2Δ
pma1-Δ916
Ec
0
2
4
6
Ec
ATP
0
0.5
1
1.5
ATP Relative Abundance

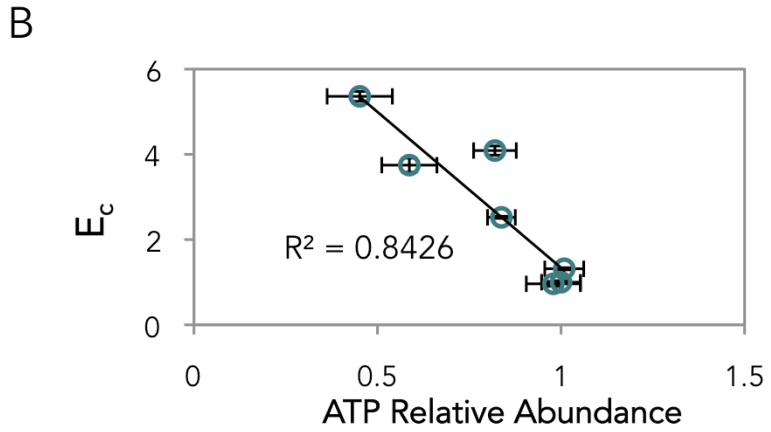
B
6
4
2
0
Ec
R² = 0.8426
0
0.5
1
1.5
ATP Relative Abundance

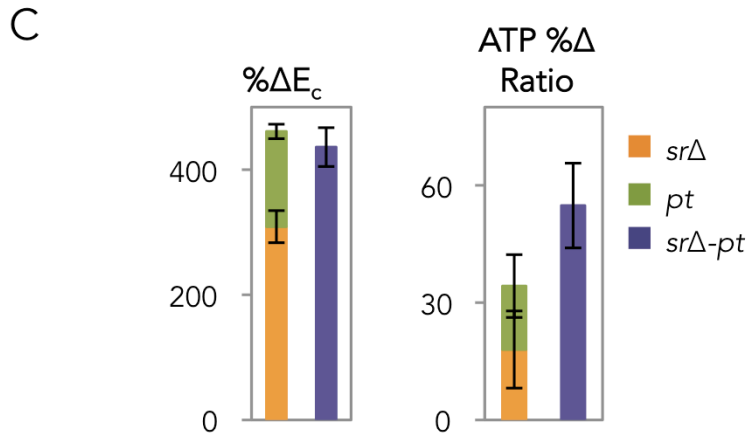
C
%ΔEc
ATP %Δ Ratio
400
200
0
60
30
0
srΔ
pt
srΔ-pt

713

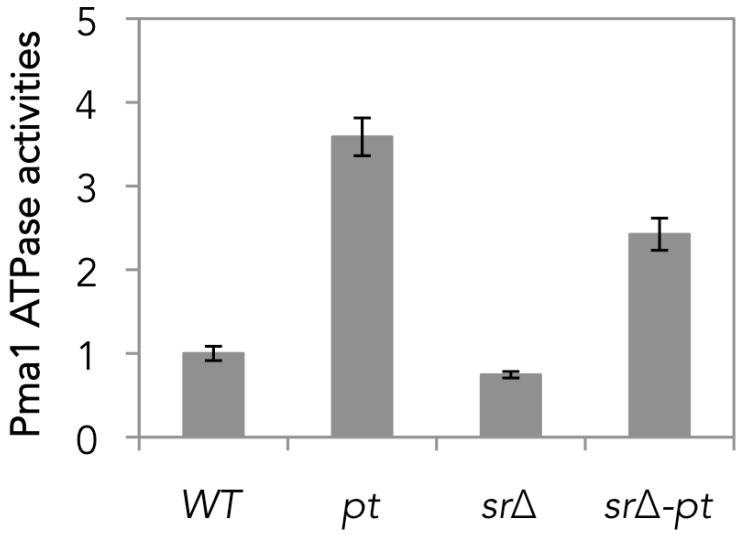

714
715

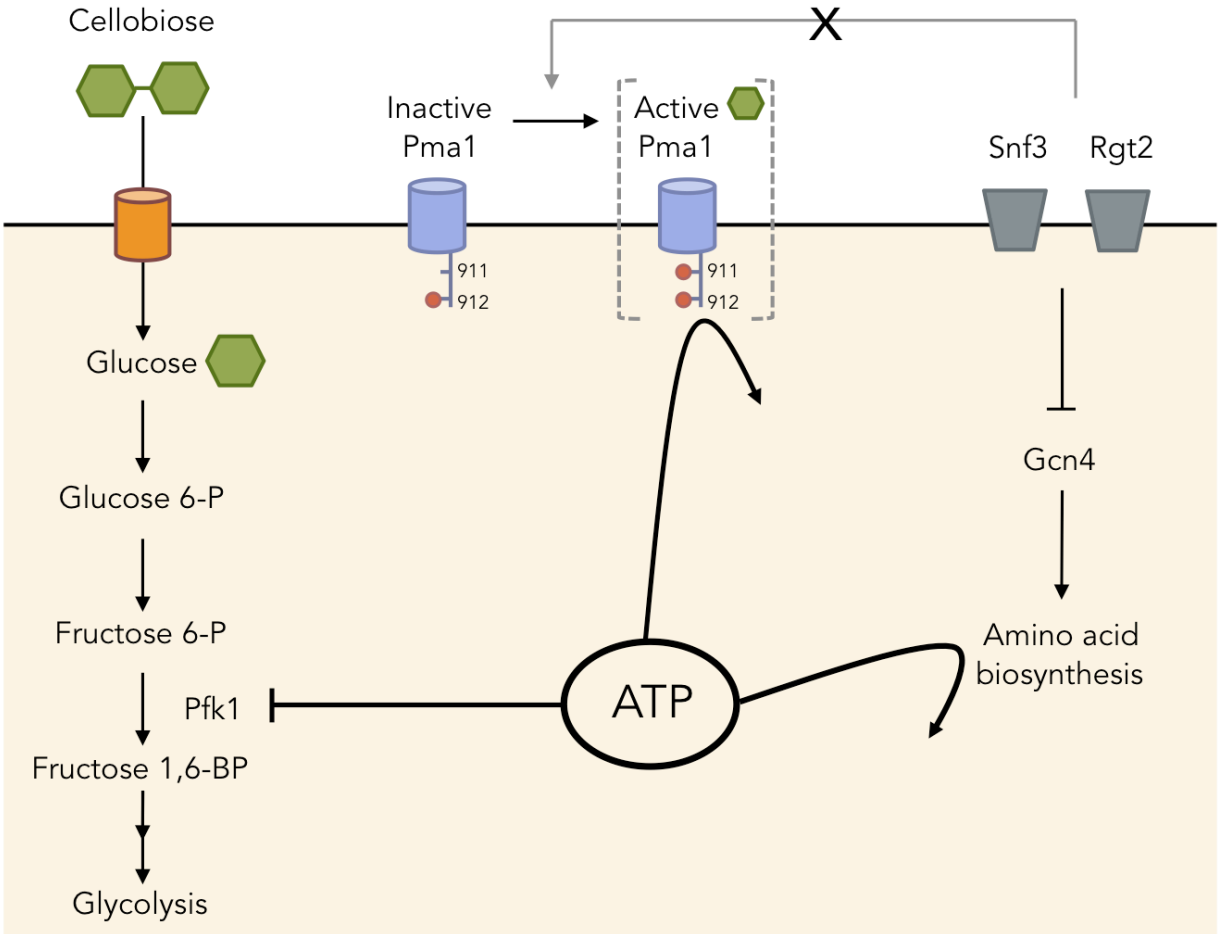
Cellobiose
X
Inactive
Pma1
Active
Pma1
Snf3
Rgt2
911
912
911
912
Glucose
Glucose 6-P
Fructose 6-P
Pfk1
Fructose 1,6-BP
Glycolysis
ATP
Gcn4
Amino acid
biosynthesis

715
716

716 **Supplementary Figures**

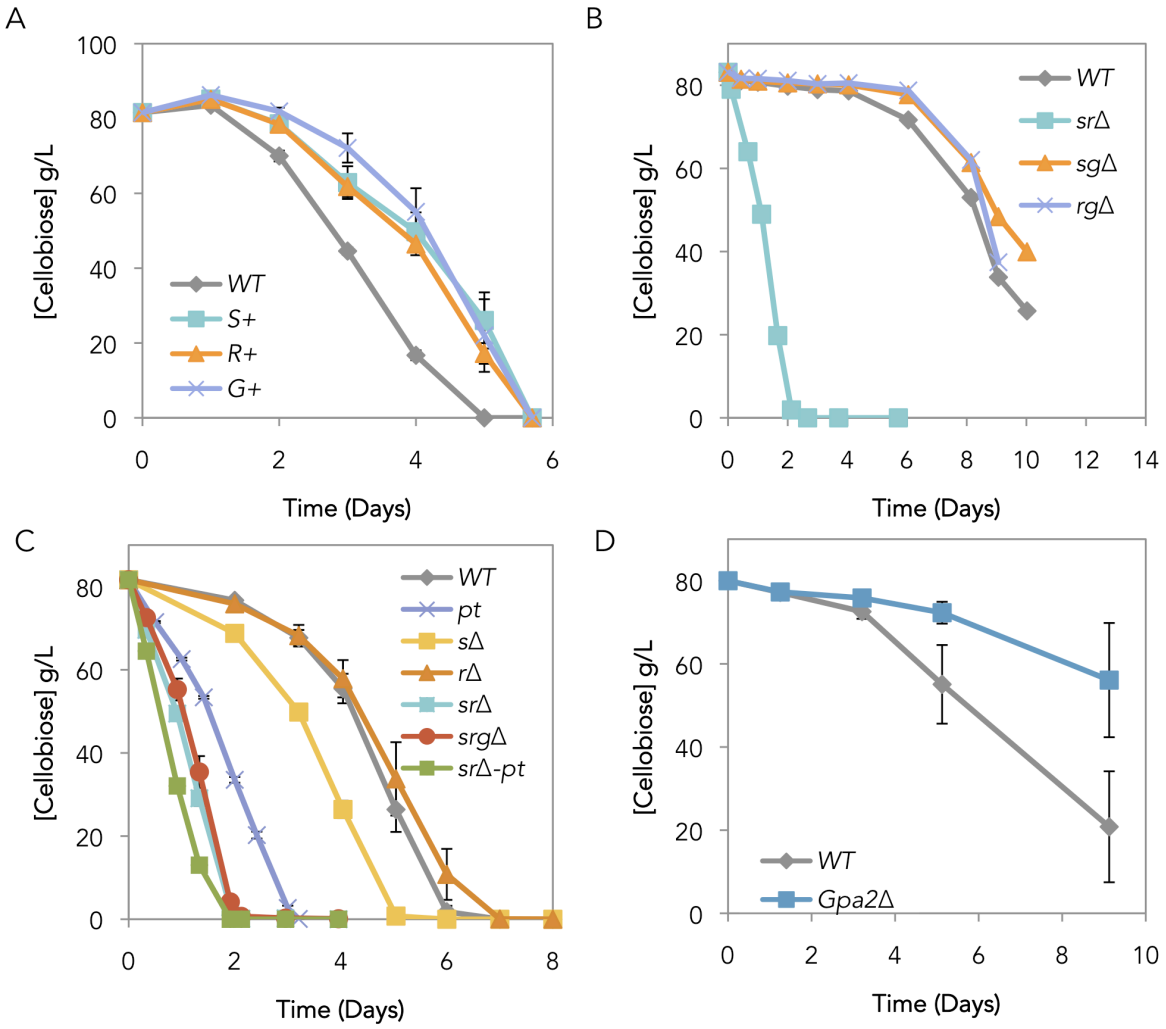

717

718 **Figure S1. Cellobiose consumption profiles and efficiency of Snf3, Rgt2 and Gpa2**

719 **mutants.** (A) Cellobiose consumption profiles of strains with consitutively active Snf3

720 (R229K), Rgt2 (R231K) and Gpa2 (R273A). (B) Cellobiose consumption profiles of

721 *SNF3*, *RGT2*, and *GPA2* double deletion combinations. (C) Cellobiose consumption

722 profiles of *SNF3* and *RGT2* single deletion in comparison to the *srΔ, srgΔ and srΔ-pt*

723 strains. (D) Cellobiose consumption profiles of *GPA2* deletion (*gΔ)* in comparison to the

724 WT strain. In panels A, B, C, and D, the results of 3 biological replicates are shown.

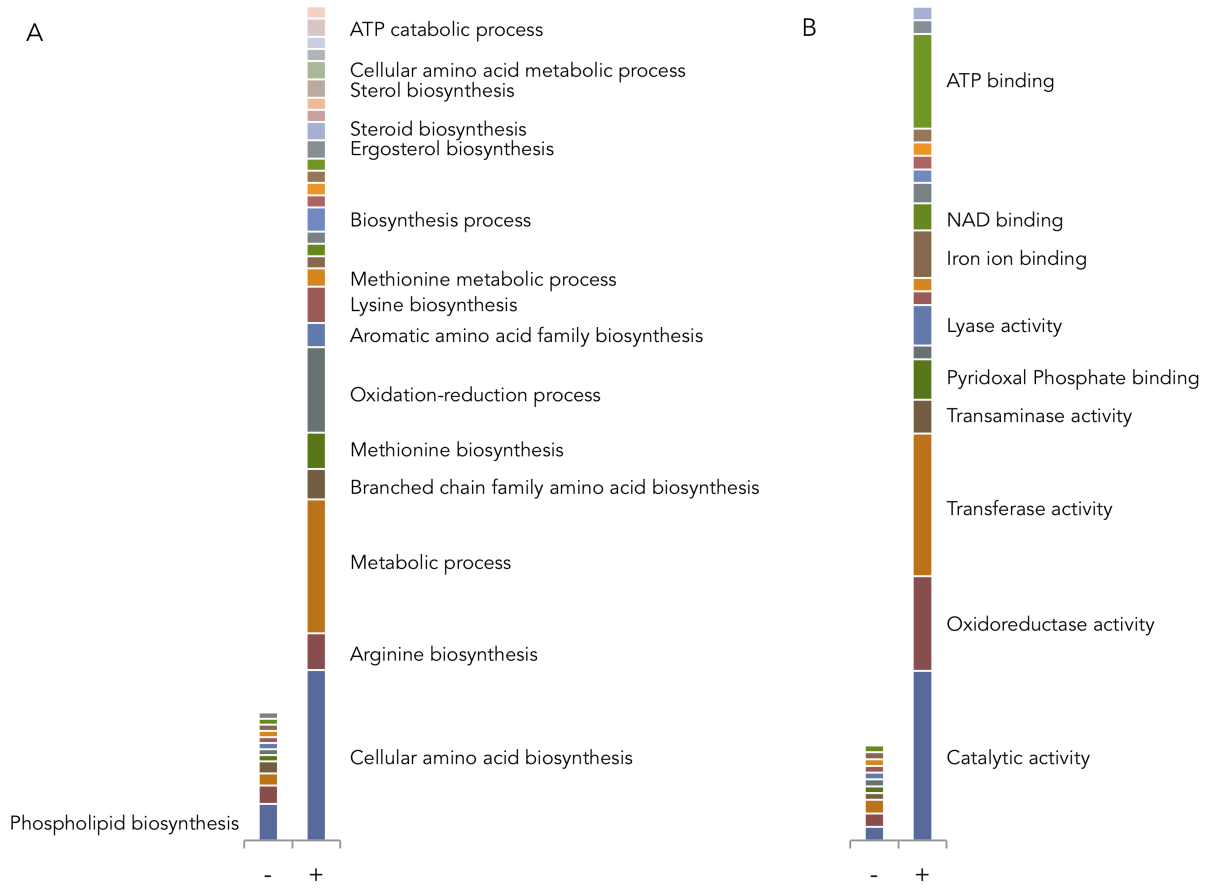

725

726 **Figure S2. Functional classification of genes uniquely expressed in the *sr*Δ strain.**

727 (A) Classification based on GO Biological Processes. (B) Classification based on

728 Molecular Function. The symbol – denotes genes which were uniquely downregulated

729 and + denotes genes which were uniquely upregulated in *sr*Δ. Catagories shown are

730 those with more than two genes detected in the cluster. Dataset 1.6 contains complete

731 classifications of the cluster.

732

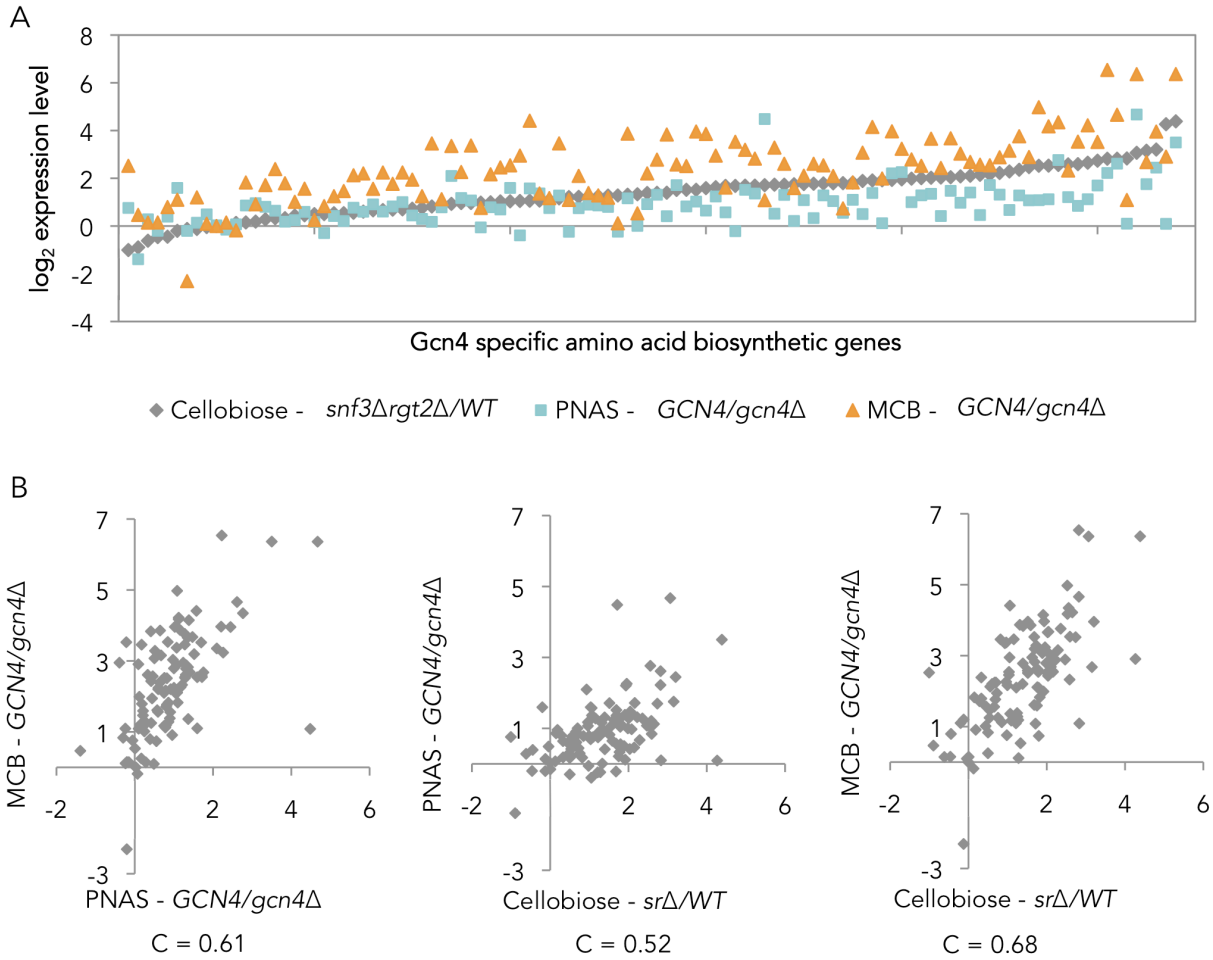

Figure S3. Gcn4-specific amino acid biosynthetic gene comparison. (A) Differential expressional levels of strains from this study (*snf3*Δ*rgt2*Δ/WT) in comparison to *GCN4*/*gcn4*Δ from Moxley *et al.,* 2009 (PNAS) (Moxley *et al*, 2009) and Natarajan *et al.,* 2001 (MCB) (Natarajan *et al*, 2001) studies. (B) Pairwise plot of expression levels from three studies and their correlations.

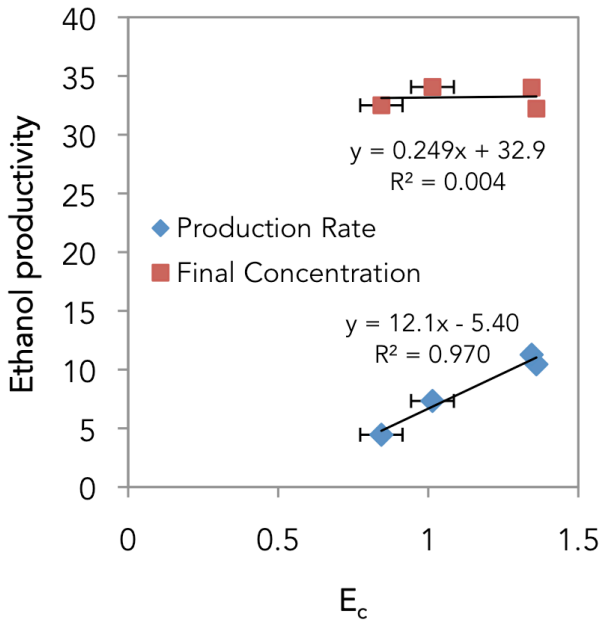

738

739 **Figure S4. Relationship of ethanol productivity parameters and cellobiose**

740 **consumption efficiency (E_c).** Ethanol production rate and the final concentration of

741 ethanol are plotted against E_c.